WATERFLOODING OPTIMIZATION USING INTELLIGENT COMPLETIONS

Kewin Passos Granados

Bernardo Horowitz

Leonardo Correia de Oliveira

kewin.passosg@ufpe.br

horowitz@ufpe.br

leonardo.oliveira@ufpe.br

Department of Civil Engineering, Federal University of Pernambuco

Rua Acadêmico Hélio Ramos, s/n, Cidade Universitária, 50740-530, Recife, PE, Brazil

Abstract. *The oil industry strives to design tools that allow greater control over wells. Flow Control Valves (FCV) are equipment installed in the bottomhole with the function of controlling the flow that enters the tubing, to handle early water (gas) breakthrough, and generate additional pressure losses in the fluid. This study makes a comparative analysis between the results obtained with the FCVs working in passive mode and working in active mode. The model was designed to improve the performance of wells with intelligent completions, to evaluate the economic return of reservoir, and to optimize the settings of the FCVs. A simple reservoir model with two wells are created, the FCVs are installed to create intelligent completions, numerical simulations are used to change the controls through setting of the FCV´s aperture, several iterations are generated to find the optimal setting of the FCVs, the reservoir was submitted to a waterflooding process. A software of wells segmentation and a numerical program are used to perform the optimization. In the passive mode, the configuration for each of the FCVs does not change over time. In active mode, the FCV setting can change in any control cycle to improve productions conditions, each new setting is generated by optimization iterations. The Sequential Quadratic Programming algorithm is chosen as the optimizer. Results show that the use of FCVs in active mode and the optimization of FCVs settings improve the production conditions and the economic return, represented by the Net Present Value (NPV).*

Keywords: *Oil reservoir, Waterflooding optimization, Intelligent completions*

INTRODUCTION

Intelligent wells are unconventional wells that have a monitoring system in real time, flux, pressure and temperature sensors; this kind of wells also have data transmission systems. It makes necessary the installation of a cables network for supply energy and communicates the sensors, fluid flow production and injection control systems (wellbore equipment) installed in the production and injection tubing and flow control valves (FCV). All these installed systems require intelligent wells that can be remotely monitored and surface controlled (Aakre, Halvorsen, & Werswick, 2013; Alsyed & Yateem, 2012; Jasen, 2001; Meshioye, Mackay, Ekeoma, & Chukuwezi, 2010). Intelligent wells have the ability of isolate and control individual zones in the reservoir (well segmentation), avoid and restrict (to exclude) production of a specific fluid in each zone; this type of wells also allow adding controlled pressure losses to the fluid that is going to enter at the tubing from the porous media, besides to operate without human intervention (Alsyed & Yateem, 2012). The different devices and monitoring systems used at intelligent wells allow greater control over the wells without unnecessary interventions, to solve unexpected problems, maximize the oil production, minimize undesirable fluids production, improve reservoir manage and increase the final recovery (Sefat & Muradov, 2013). Intelligent wells, because of their versatility and flexibility, could work in different scenarios more efficiently than conventional wells. Some applications examples of this wells are water or gas shut-off, fluid transfer, oil rims in single compartments, gas coning, commingled production and heel-Toe effect.

Water or gas shut-off: water and gas breakthrough does not occur simultaneously in all zones or layers where the well cross due to differences in permeability in reservoir; when are used intelligent terminations at each interval it is possible to close each well segment with an water or gas breakthrough, decreasing the amount of this undesirable fluid in the surface and preventing an anticipated closure of the well (Jasen, 2001).

Fluid transfer: smart wells can connect an oil reservoir with a high-pressure gas or water zone underlying, where pressure sensors and flow control devices installed in the injector interval allow fluid transfer of dump flooding in a controlled way in order to pressurize the oil reservoir, supply it with greater energy for its production and improve its sweep efficiency (Glandt & E, 2005; Jasen, 2001).

Oil rims in single compartments: a completed well in a thin oil column between the oil/water contact and gas/oil contact may suffer an early breakthrough of water or gas in the heel if the pressure losses over the entire well length is comparable to the drawdown in the heel; oil production declines abruptly due to excessive amount of water, this fluid flow behavior leads to a premature well closure. A timely implementation of flow control devices in the horizontal well can generate additional pressure losses in the fluid along the well with the purpose to equalize the pressure inside the tubing and improve the production profile in whole the horizontal well (Glandt & E, 2005).

Gas coning: occurs when the gas/oil contact moves toward the well as a result of the oil drawdown; At a given time in the production life the gas/oil contact will reach the producing well and the gas breakthrough must occur, make gas phase to dominate the production. The breakthrough has negative effects like damage to equipment that does not support large amounts of gas, the well is no longer workable (uneconomical), the reservoir is fastest depleted losing instantly its energy. Flow control devices may control the production flow rate in zones where the gas coning is occurring thus preventing gas breakthrough (Leemhuis, Belfroid, Alberts, & Science, 2007).

Commingled production: The flow control devices allow a commingled production by a single well of zones with different pressures and permeabilities, through the impact of the influx of the most pressurized zone with a continuously variable device, it avoid a cross-flow towards the less permeable zone. Benefits of using smart terminations range from performing fewer well interventions to the absence of workover, which means an optimization of net surface oil production, accelerated production, production of different zones at the same time, or maintaining a surface constant production if there are reservoir restrictions (Glandt & E, 2005; Jasen, 2001).

Heel-Toe effect: Pressure losses produced along a horizontal well means that the flow pressure of the production tubing is lower at the heel of the well than at the toe. Over time, long before oil coming from sections near the toe reaches the well, the water or gas front will reach the heel of the well causing a breakthrough of these undesirable fluids and leaving the oil confined in the toe section without being able to be produced; this leads to the anticipated end of the productive well life. The flow control devices equalize the pressure drop produced throughout the entire well, stimulating the uniform oil flow through the formation so the water and gas fronts are delayed preventing an early breakthrough of these fluids (Ellis et al., 2010).

1 HARDWARE

FCV are equipments in the well bottom (tubing) and can be remotely operated from surface by hydraulic or electric systems or the combination of both, which sends an energy pulse to configure the position of the valve (Flow area) (Al-khelaiwi, Birchenko, Konopczynski, & Davies, 2010; Williamson, Bouldin, & Purkis, 2000). The device orifice diameter can be remotely adjusted to decrease or increase the fluid flow by choking depending on the production conditions. Additionally, the water or gas production can be completely stopped in reservoir zones where there is a breakthrough point of these undesirable fluids (Aakre et al., 2013; Rahman, Allen, & Bhat, 2012). These valves exist in a wide range of commercial designs with the widest range of functionality to control more flow regimes. These designs can be found from a simple on/off system to an infinitely variable system (Al-khelaiwi et al., 2010). FCVs may require to move under high pressure and high temperature conditions (HP - HT), or in significant fluctuations of these, consequently it is necessary that FCVs are sufficiently robust and reliable without compromising their functionality (Rahman et al., 2012).

In general, FCV design comprises a Top Sub, balanced hydraulic piston, Seat Assembly, Lower Seat Assembly (with Valve Flow Trim), and Bottom Subassembly. The Top Sub provides structural integrity and the hydraulic piston chambers is lodge in it. The application of differential pressure through the hydraulic piston drives the movement of the upper seat assembly. This movement of the assembly disengages the upper seat from the lower seat and allows fluid flow and communication between the annulus and the tubing. The flow trim has a flow profile cut into it to provide the desired flow characteristics. Hydraulic pressure (or electrical signal) is applied through control lines to each side of the hydraulic piston to move the valve in any direction. The valve can then be opened or returned to the closed position by applying pressure to the control lines (Rahman et al., 2012).

2 MODEL FORMULATION

2.1 Field model and reservoir description

The studied model is a segmented synthetic reservoir that is composed of different layers; it has a water injector well and a vertical drilled producer well throughout the reservoir thickness. The model was built with 15 blocks in x-direction, 15 blocks in y-direction, and 3 layers, these used in the vertical direction; it gives a total of 675 blocks. Each cell has a size of 30,5x30,5x15,25 m, resulting in a total reservoir extension of 457,2x457,2 m and a thickness of 45,72 m. During the 10 years of concession period, the reservoir is under a water injection process. The reservoir top is at a depth of 2.735,6 m. The upper layer of the reservoir has a horizontal permeability of 100 mD (9,87e-14 m²) with a porosity of 0,15; The lower layer has a horizontal permeability 10 times greater than the upper layer with the same porosity. Unlike the upper and lower layers, the reservoir middle layer does not present transmissibility, so this layer could be considered a flow barrier, separating the more permeable layer of the reservoir from the less permeable. The vertical permeability of the reservoir is constant at 10 mD (9,87e-15 m²).

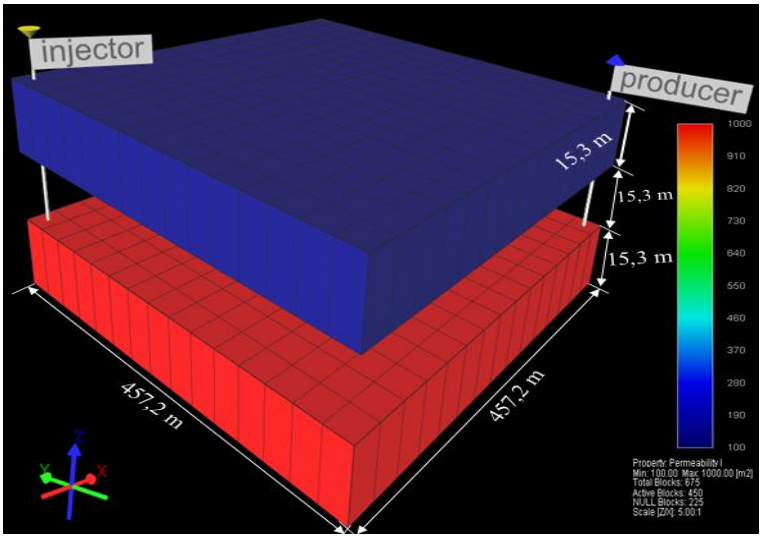

Figure 1. reservoir model and dimensions

2.2 Setting wellbore model

Two wells are considered, a conventional injector well, which supplies energy for both layers (upper and lower); The well has 2.781,3 m of total vertical depth. In the upper layer, water is injected through the opening in the tubing, that is located at 2.743,2 m. In the lower layer, the water is injected through the tubing end open to flow. To isolate the injection zone a packer was installed in the well at a depth of 2.735,6 m. The producer well is a vertical segmented well, with a depth of 2.781,3 m, completed in the two producing zones. At each zone, an FCV was installed to control the reservoir flow that is coming into the tubing. The device installed in Zone A (less permeable) is located at a depth of 2.743,2 m, and the device installed in Zone B is at a depth of 2.773,7 m; Two packers were installed in the well, the first at a depth of 2.735,6 m, the second at a depth of 2.758,4 m, to isolate the low permeability zone of high permeability zone and thus prevent one zone having influence or interference on the other one. Table 1 summarizes the main characteristics of the model.

Table 1. Model features

Parameter	Value
Average initial pressure	41,73 kPa
Horizontal permeability at the Zone A	100 mD
Horizontal permeability at the Zone B	1.000 mD
Vertical permeability of the reservoir	10 mD
Reservoir porosity	15%
Rock compressibility	1×10^{-6} (kgf/cm^2)
Simulation mesh	$15 \times 15 \times 3$

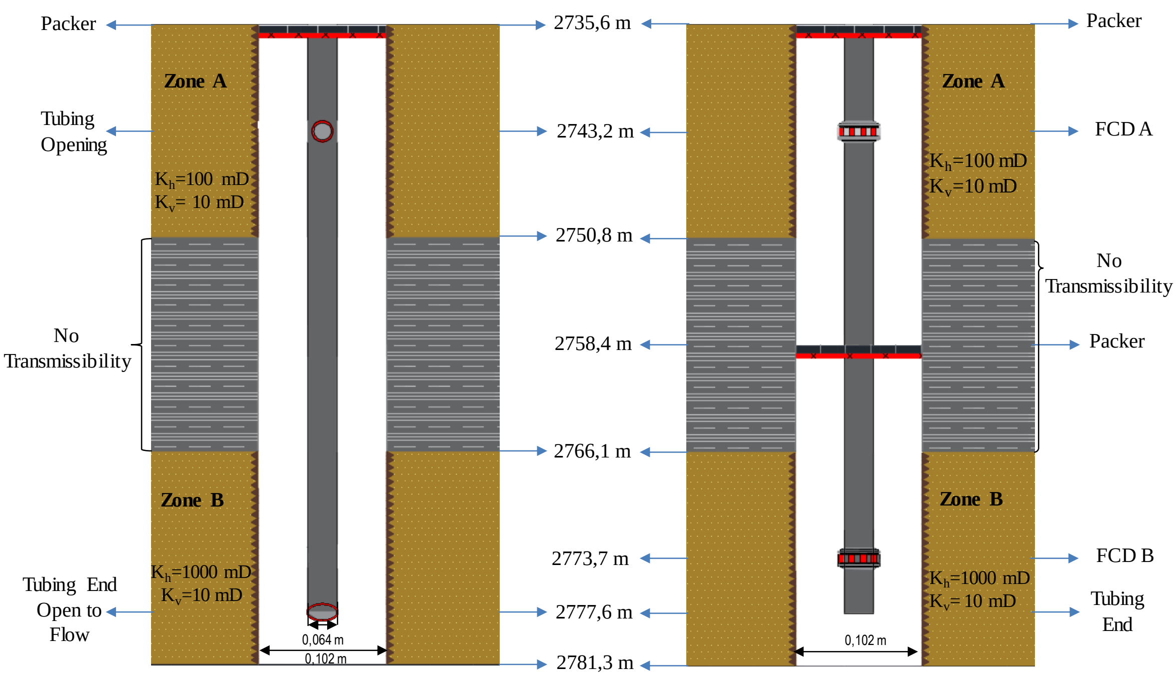

Figure 2. Well configurations. (a) injector well with a constant injection rate of 318 m³/day, the well location is (i,j,k) 1,1,1:3. (b) producer well located (i,j,k) 15,15,1:3

2.3 Inflow control strategies and setting FCVs

In this section of the work a description of the FCVs installed in the producing well and of the strategies used to simulate the model is made, making a comparative analysis between the results obtained with the devices working in passive mode and working in active mode. The model was designed to improve the performance of wells with intelligent completions, to evaluate the economic return of the reservoir, to optimize the settings of the installed devices and to create a base for the development of intelligent wells that can be implemented in scenarios more complex and realistic situations. The main objective of this study is to lay the foundations for, in the near future, to create and optimize control policies for the openings of the installed devices in both horizontal and vertical wells, and that they can react at the right moment to unexpected conditions of production, such as early water or gas breakthrough, a sudden increase in these unwanted fluids, cross flow between formations with different petrophysical characteristics, etc., which are caused by uncertainties in the reservoir near the well.

Case Base: in the passive case, the orifice diameter of the two devices installed in the producer well, like the rest of the parameters, remain constant throughout the time, without any modification in their values; the two devices remain with the diameter fully open in their entirety throughout the simulation time in order to evaluate the commingled production of the layers.

Controlled Case: in the active case, unlike the passive case, the orifice size of each device can change as the production conditions change, the device opening can increase or decrease in each control cycle when the situation warrants it, and each device can change its diameter independently of the other device's setting to improve oil production and restrict water production, just as in the passive case the other parameters will remain constant over time. The diameter controls of each device are optimized according to the production conditions, in order to recover as much oil as possible, producing the least amount of water, and thus increase the net present value (NPV) of the reservoir.

Table 2. Device operational parameters at base case

Base Case						
Parameter	Inlet Diameter	Orifice Diameter	Outlet Diameter	Operating Temperature	Ratio C_p/C_v	Discharge Coefficient
Value	0,064 m	0,013 m	0,064 m	80 °C	1,4	0,85

The producer well was segmented using the iSegWell module of CMG (CMG, 2016b) and the simulation of each scenario was performed in the commercial IMEX software (CMG, 2016a) in conjunction with a numerical program that performed the optimization of the device openings in certain time steps. Table 2 and Table 3 shows the parameters and settings of the devices installed in the production well for each case.

Table 3. Device operational parameters at controlled case

Controlled Case						
Parameter	Inlet Diameter	Orifice Diameter	Outlet Diameter	Operating Temperature	Ratio C_p/C_v	Discharge Coefficient
Value	0,064 m	dynamic	0,064 m	80 °C	1,4	0,85

Table 4. Values used in the NPV calculation

Oil Price	$ 25/m^3
Produced Water Cost	$ 5/m^3
Injected Water Cost	$ 2/m^3
Discount Rate	0,093

2.4 Production constraints and variables

The project variables under consideration are the orifice diameters of each flow control valve; The variables are normalized to operate in a range of 0,1 to 1, where the value of 1 represents that the orifice is fully open and 0,1 represents an opening of 10% in the orifice diameter. The variables are normalized by dividing the diameter of the device of zone "z" at time "t" by the maximum diameter allowed for each device.

$$x_{z,t} = \frac{DV(z,t)}{MDV} \quad (1)$$

Where $DV(z,t)$ is the orifice diameter of the valve in the zone " z " in the time interval "t" , MDV is the maximum diameter allowed for each valve, and $x_{z,t}$ is the normalized variable of the zone " z " in the time interval " t ".

2.5 Objective function

The objective function to be evaluated and maximized in this study is the net present value (NPV) of the reservoir, which represents a mathematical-financial function whose purpose is to determine the present value of future payments taking into account a discount rate. Basically, it is the cash flow of the reservoir, and it is equivalent to the calculation of how much the future payments would be currently valid (Oliveira, 2013). The NPV is a function of the current price of the oil unit, the cost of treatment of the unit of water produced, the cost of each unit of injected water, also takes into consideration the liquid production flow rates and the water injection flow rates, in addition to the discount rate applied to capital, among other parameters (Horowitz, Bastos, & Mendonça, 2013; Oliveira, 2013). The equation that calculates the NPV can be expressed as

$$VPL = \sum_{t=0}^{T} \left[\frac{1}{(1+d)^t} * F(q_t) \right] \tag{2}$$

Where d is the discount rate, T is the total operating time, $F(q_t)$ is the cash flow in the time "t", given by the following equation

$$F(q_t) = \sum_{P=1}^{nP} \left(r_o q_{p,t}^{o} - c_w q_{p,t}^{w} \right) - \sum_{I=1}^{nI} \left(c_{wi} q_{I,t}^{w} \right) \tag{3}$$

Where P and I are the indicators of producer and injector wells respectively, nP is the total number of producer wells, nI is the total number of injector wells, r_o is the oil price, $q_{p,t}^{o}$ and $q_{p,t}^{w}$ are the average flows of oil and water production respectively, c_w is the cost of producing water, c_{wi} is the cost de injecting water (Horowitz et al., 2013). Table 4 are the prices and values used for the calculation of the NPV

2.6 Problem formulation

To optimize the problem, we subdivide the reservoir concession period into five control cycles each with a fixed duration time as shown in Fig. 3. In each control cycle an evaluation of the production conditions of the well is made to decide the size of operation of the orifice.

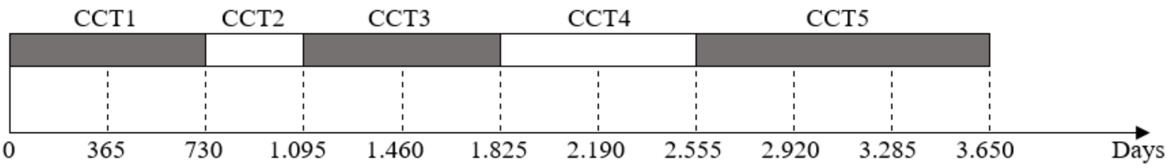

Figure 3. Control cycles with defined fixed times

CCT(i) is the abbreviation for Control Cycle Time, which represents the division and duration of each control cycle.

After defining the project variables, the objective function, and establishing the control cycles, we can formulate the problem to be optimized mathematically as:

$$\text{Maximize} \qquad NPV = \sum_{t=0}^{T} \left[\frac{1}{(1+d)^t} * F(q(x_{z,t})_{p,t}) \right]$$

$$\text{Subject to:} \qquad 0.1 \le x_{z,t} \le 1 \tag{4}$$

2.7 Pressure drop models

Pressure drop through of the device: The flow rate through an orifice increases when the pressure difference between the upstream and the downstream ends of the orifice increases, similarly for any flow control device, that increase in flow rate will occur until the critical pressure difference is reached, since this critical pressure difference defines the maximum (or critical) flow rate for the orifice (CMG, 2016b). If the upstream pressure (P_{up}) remains constant, then the mass flow rate is only a function of the downstream pressure (P_{down}) when it is in the subcritical flow region, and when the pressure difference reaches the critical value the mass flow rate will be independent of the downstream pressure (Perkins, 1993). An equation is formulated that calculates the maximum (critical) mass flow rate through a device, which is a function of flow conditions, device geometry, upstream pressure, and the relationship between downstream pressure and upstream pressure (P_R). The critical flow rate occurs when P_R is less than the critical pressure ratio, P_R^*. As the critical pressure ratio, P_R^*, defines the maximum flow rate, then we can evaluate it from a maximum mass flow rate possible as follows:

$$\frac{d(q_m)}{d(P_R)} = 0 \tag{5}$$

Where q_m is the mass flow rate, and P_R is the relationship between downstream pressure and upstream pressure.

The mass flow rate in subcritical flow can be calculated as follows:

$$q_m = \left[\frac{2 \cdot P_{up} \cdot \rho_{mix} \cdot \left(\lambda \cdot \left(1 - P_R^{\frac{k-1}{k}}\right) + \alpha \cdot (1 - P_R)\right)}{\left(f_g \cdot P_R^{\frac{-1}{k}} + \alpha\right)^2 - \left(\frac{A_{orif}}{A_{up}}\right)^2 \cdot \left(f_g + \alpha\right)^2}\right]^{0.5} \tag{6}$$

Where P_{up} is the upstream pressure, ρ_{mix} is the mass density of mixture, k is the ratio of mixture heat capacities at constant pressure to constant volume (C_p/C_v), f_g is the mass fraction of gas, A_{orif} and A_{up} are the orifice and upstream area, respectively.

$$\alpha = \rho_{mix} \cdot \left(\frac{f_o}{\rho_o} + \frac{f_w}{\rho_w}\right) \tag{7}$$

$$\lambda = f_g + \frac{\left(f_g \cdot c_{vg} + f_o \cdot c_{vo} + f_w \cdot c_{vw}\right) \cdot M}{Z \cdot R} \tag{8}$$

Where f_o and f_w are respectively the mass fraction of oil and water, ρ_o and ρ_w are the mass density of oil and water, c_{vg}, c_{vo}, and c_{vw} are the heat capacities of gas, oil and water at constant volume, M is the molecular mass of gas, Z is the compressibility factor of the gas, and R is the gas constant.

Then the volumetric critical flow can be calculated as:

$$Q^* = \frac{A_{orif} \cdot C_D \cdot {q_m}^*}{\rho_{mix}} \tag{9}$$

Where C_D is the discharge coefficient, ${q_m}^*$ is the critical flow.

In the iterative scheme using the simulator, the upstream pressure and the mass flow rate are treated as known values, and the downstream pressure is the main unknown of the problem (CMG, 2016b). When the mass flow is equal to or less than the critical value, then the flow is treated as subcritical and empirical correlations are used to calculate the downstream pressure; an elliptic approximation is used to correlate the pressure ratio against the flow rate in current and critical condition (Boone, Youck, & Sun, 2001).

$$P_R = {P_R}^* + (1 - {P_R}^*) \cdot \left[1 - \left(\frac{Q}{Q^*}\right)^2\right]^{0.5} \tag{10}$$

Where ${P_R}^*$ the critical pressure ratio, Q is the actual flow rate.

Using the Perry's relation (R. H. Perry & Green, 2007) for subcritical flow, we obtain:

$$P_{down} = P_{up} \cdot \left[1 - (1 - P_R) \cdot \left[1 - \left(\frac{d_{orif}}{d_{down}}\right)^{1.85}\right]\right] \tag{11}$$

Where P_{down} is the downstream pressure, d_{orif} and d_{down} are the downstream and orifice diameter.

That represents the correlation between the pressures at points before and after the orifice of the device and its geometry as a function of the relation of pressures.

Pressure losses in the well: To calculate the pressure loss of the fluid along the producer well was used the Drift-Flux model, which is a homogeneous model that considers slip between the phases, each phase is considered separately, allowing to calculate different velocities for each phase. The model is formulated in terms of equations of conservation of mass, momentum and energy of each phase. In the Drift-Flux model it is assumed that the two-phase dynamics can be expressed by the mixture-momentum equation with the constitutive kinematic equation by specifying the relative motion between the phases. In the Drift-Flux model, the velocity fields are expressed in terms of the mixture-center-of-mass velocity and the drift velocity of the gas phase, the latter being the gas velocity with respect to the volume center of the mixture (Hibiki & Ishii, 2003; Soprano, Ribeiro, Silva, & Maliska, 2010). In this section, we will present equations and basic formulas for a two-phase flow model in one direction. In this case it is considered that all properties in each control volume along the well do not vary in any direction. In order to obtain the model in one direction it is essential to integrate all properties over a cross-sectional area, and thus to introduce appropriate mean values. A simple area average of a property over a cross-sectional area can be defined as:

$$\langle \theta \rangle = \frac{1}{A} \int \theta \, dA \tag{12}$$

Where θ is any definite property and A is the cross-sectional area. It is also important to define the volumetric fraction of each phase (f_α), which represents the relation between the volume occupied by the phase α and the total volume of the system. Assuming that throughout the control volume the properties do not vary, the volumetric fraction can be calculated as the ratio between the cross-sectional area occupied by the phase and the total area.

$$\langle f_\alpha \rangle = \frac{V_\alpha}{V} = \frac{A_\alpha}{A} \tag{13}$$

Where $\langle f_\alpha \rangle$ is the average fraction of each phase, V_α is the volume occupied by phase, A_α is the cross-sectional area occupied by the phase, V is the total control volume, and A is the total area. The sum of the volumetric fraction of each of the phases must be equal to one. The density of each phase, ρ_α, within any cross-sectional area is considered uniform, so it can be expressed as follows:

$$\rho_\alpha = \langle\langle \rho_\alpha \rangle\rangle \tag{14}$$

Under the above assumption, the average density of the mixture is given by

$$\langle \rho_m \rangle \equiv \langle f_g \rangle \rho_g + (1 - \langle f_g \rangle)\rho_l \tag{15}$$

Where $\langle f_g \rangle$ is the average fraction of gas, ρ_g is the gas density and ρ_l is the liquid density.

Then the mixture velocity is defined

$$\overline{v_m} = \frac{\langle f_g \rangle \rho_g \langle\langle v_g \rangle\rangle + \langle f_l \rangle \rho_l \langle\langle v_l \rangle\rangle}{\langle \rho_m \rangle} \tag{16}$$

Where $\langle\langle v_g \rangle\rangle$ is the gas velocity, $\langle\langle v_l \rangle\rangle$ is the liquid velocity and $\langle \rho_m \rangle$ is the average mixture density.

And the volumetric flow is given by

$$\langle j \rangle \equiv \langle j_g \rangle + \langle j_l \rangle = \langle f_g \rangle \langle\langle v_g \rangle\rangle + \langle f_l \rangle \langle\langle v_l \rangle\rangle \tag{17}$$

Where $\langle j_g \rangle$ is the gas volumetric flow, $\langle f_l \rangle$ is the average fraction of liquid, and $\langle j_l \rangle$ is the liquid volumetric flow.

The drift velocity of the gas phase is defined as the velocity of the dispersed phase with respect to the volume center of the mixture. The appropriate average drift velocity is defined by

$$\overline{V_{gJ}} = \frac{\langle j_g \rangle}{\langle f_g \rangle} - (\langle j_g \rangle + \langle j_l \rangle) \tag{18}$$

Based on the definitions of velocity fields, expressions for calculating the velocity of each phase can be obtained as follows

$$\langle\langle v_g \rangle\rangle = \frac{\overline{v_m} \langle \rho_m \rangle + \rho_l \overline{V_{gJ}}}{\langle \rho_m \rangle} \tag{19}$$

$$\langle\langle v_l \rangle\rangle = \frac{\overline{v_m}\langle f_l \rangle\langle \rho_m \rangle - \langle f_g \rangle \rho_g \overline{V_{gJ}}}{\langle f_l \rangle\langle \rho_m \rangle} \tag{20}$$

$$\langle j \rangle = \frac{\overline{v_m}\langle \rho_m \rangle + \langle f_g \rangle(\rho_l - \rho_g)\overline{V_{gJ}}}{\langle \rho_m \rangle} \tag{21}$$

The two-phase Drift-Flux model will be extended to a three-phase flow model, considering that the liquid phase is a mixture of two fluids, water and oil, and the model for three phases with new parameters will be applied again, in addition it will be assumed in this new case that the oil is dispersed in the water (Hibiki & Ishii, 2003; Soprano et al., 2010)

$$\overline{V_{ow}} = \frac{\langle j_o \rangle}{\langle f_o \rangle} - (\langle j_o \rangle + \langle j_w \rangle) \tag{22}$$

Where $\langle j_o \rangle$ is the oil volumetric flow, $\langle f_o \rangle$ is the average fraction of oil, and $\langle j_w \rangle$ is the water volumetric flow. The oil velocity is defined as

$$\langle\langle v_o \rangle\rangle = \frac{\overline{v}_l\langle \rho_l \rangle + \rho_w \overline{V_{ow}}}{\langle \rho_l \rangle} \tag{23}$$

Where $\overline{v}_l$ is the liquid velocity, $\overline{V_{ow}}$ is the average drift velocity of the oil, and ρ_w is the water density.

$$\langle\langle v_w \rangle\rangle = \frac{\overline{v}_l\langle f_w \rangle\langle \rho_l \rangle - \langle f_o \rangle \rho_o \overline{V_{ow}}}{\langle f_l \rangle\langle \rho_m \rangle} \tag{24}$$

Where $\langle f_w \rangle$ is the average fraction of water.

In this presented model, we need to solve four equations to calculate all the necessary properties, three continuity equations and one moment equation.

Mixture Continuity Equation

$$\frac{\partial\langle \rho_m \rangle}{\partial t} + \frac{\partial(\langle \rho_m \rangle\overline{v_m})}{\partial s} = \left(\frac{\dot{m}}{V}\right)_{total} \tag{25}$$

Mixture Momentum Equation:

$$\frac{\partial(\langle \rho_m \rangle\overline{v_m})}{\partial t} + \frac{\partial(\langle \rho_m \rangle\overline{v_m v_m})}{\partial s} = -\frac{\partial P}{\partial s} - \langle \rho_m \rangle \cdot g \cdot sin(\theta) - \frac{f}{2D}\langle \rho_m \rangle\overline{v_m}|\overline{v_m}| - \frac{\partial}{\partial s}\left(\frac{\langle f_g \rangle \rho_g \rho_l}{\langle f_l \rangle\langle \rho_m \rangle}\overline{V_{gJ}}^2\right) \tag{26}$$

Gas Phase Continuity Equation**:**

$$\frac{\partial\left(\langle f_g\rangle\rho_g\right)}{\partial t}+\frac{\partial\left(\langle f_g\rangle\rho_g\overline{v_m}\right)}{\partial s}=\left(\frac{\dot{m}}{V}\right)_g-\frac{\partial}{\partial s}\left(\frac{\langle f_g\rangle\rho_g\rho_l}{\langle\rho_m\rangle}\overline{V_{gJ}}\right) \quad (27)$$

Oil Phase Continuity Equation:

$$\frac{\partial(\langle f_o\rangle\rho_o)}{\partial t}+\frac{\partial(\langle f_o\rangle\rho_o\overline{v_m})}{\partial s}=\left(\frac{\dot{m}}{V}\right)_o-\frac{\partial}{\partial s}\left(\frac{\langle f_o\rangle\rho_o\rho_w}{\rho_l}\overline{V_{ow}}\right)+\frac{\partial}{\partial s}\left(\langle f_o\rangle\rho_o\frac{\langle f_g\rangle}{\langle f_l\rangle}\frac{\rho_g}{\langle\rho_m\rangle}\overline{V_{gJ}}\right) \quad (28)$$

Where $(\dot{m}/V)_\alpha$ correspond to the source/sink of each phase associated with the inflow or outflow of fluids between well and reservoir, f is the fanning friction factor. This problem is solved for pressure (P), mixture velocity ($\overline{v_m}$), gas volumetric fraction ($\langle f_g\rangle$) and oil volumetric fraction ($\langle f_o\rangle$).

2.8 Setting numerical simulation

The Sequential Approximate Optimization (SAO) strategy is used to optimize the project as a sequence of local problems and the Sequential Quadratic Programming (SQP) algorithm was chosen to solve each local problem.

Sequential Approximate Optimization: This methodology is used to decompose the original optimization problem into a sequence of subproblems, which are small sub-regions of the project domain; Each sub-region is managed adaptively by the SAO strategy (Alexandrov, Dennis, Lewis, & Torczon, 1998; Eldred, Giunta, Collis, Alexandrov, & Lewis, 2004; Horowitz et al., 2013). Surrogate functions are created from evaluations in the real function and are operated by the optimization algorithm in small regions of the optimization design space, called trust regions (Horowitz et al., 2013; Oliveira, 2013). Mathematically we can define each subproblem as:

$$\begin{aligned} &\text{Minimize} && \hat{f}^k(x) \\ &\text{Subject to:} && \hat{g}_i^k(x)\leq 0,\quad i=1,\dots,m \\ &&& \boldsymbol{Ax}=\boldsymbol{b} \\ &&& \left\|\boldsymbol{x}-\boldsymbol{x_c^k}\right\|\leq\Delta^{\boldsymbol{k}} \\ &&& \boldsymbol{x_l}\leq\boldsymbol{x}\leq\boldsymbol{x_u} \end{aligned} \quad (29)$$

Where $\hat{f}^k(x)$ and $\hat{g}_i^k(x)$ are the objective-surrogate function and the m surrogate restriction functions, respectively, for iteration k, $\boldsymbol{A}$ and $\boldsymbol{b}$ represent the matrix and the vector of independent terms of the linear constraints, $\boldsymbol{x_c^k}$ is the central point of the trust region in iteration k, $\Delta^{\boldsymbol{k}}$ is the size of the trust region in the current iteration, $\boldsymbol{x_l}$ and $\boldsymbol{x_u}$ are the minimum and maximum limits, respectively, of the design variables. Each subproblem represents an SAO iteration, and in each iteration the candidate points to be optimal are validated with a fidelity model in the center of the trust region, if there is a considerable decrease then the trust region is refocused in this new point. Depending on the result obtained and the accuracy of the surrogate model, the new trust region can be extended, maintained or decreased (Horowitz et al., 2013). The SAO strategy can be summarized schematically (Giunta & Eldred, 2000):

Step 1. Calculate the objective function and constraints in the sample regions designated for the surrogate model construction.

Step 2. Construct the surrogate model for the objective function and the nonlinear constraints.

Step 3. Optimize the surrogate objective function subject to the nonlinear surrogate constraints and the original linear constraints within the trust region.

Step 4. With the optimal point found in the previous step, calculate the objective function and the original constraints.

Step 5. Verify convergence.

Step 6. Move, maintain, increase, reduce trust region according to approximate model accuracy compared to objective function values and original constraints.

Step 7. Return to step 1.

Sequential Quadratic Programing: is one of the main methods used for the numerical resolution of optimization problems with non-linear constraints; SQP is an iterative methodology that models nonlinear problems based on a given solution $\boldsymbol{x}^{(\boldsymbol{k})}$, by means of a quadratic programming (QP) subproblem, solves the QP subproblem and uses that solution to construct a new and best approximation $\boldsymbol{x}^{(\boldsymbol{k+1})}$. The methodology is performed in such a way that it creates a sequence of approximate solutions of each QP subproblem at each iteration and converges to a local minimum of the nonlinear problem (Vanderplaats, 1984). The SQP algorithm is implemented in the optimization of nonlinear problems with the following form

$$\begin{aligned} &\text{Minimize} && f(x) \quad x \in \mathrm{IR}^{\mathrm{n}} \\ &\text{Subject to:} && h_i(x) = 0, \quad i = 1, \dots, n \\ & && g_j(x) \leq 0, \quad j = 1, \dots, m \end{aligned} \tag{30}$$

Where $f(x)$ is the objective function, $h_n(x)$ and $g_m(x)$ are the n and m constraint functions of equality and inequality respectively. The set of points satisfying the constraints of equality and inequality is called the viable region of the non-linear problem, and can be defined as

$$\Gamma \coloneqq \{ x \in \mathrm{IR}^n \mid h_i(x) = 0, \ \ g_j(x) \leq 0 \}$$

And its elements are defined as feasible points. We can define in general the main stages of the SQP algorithm as:

Step 1. Define the starting point (initial point), $\boldsymbol{x}^{(\boldsymbol{0})}$.

Step 2. Configure the initial approximation for the Hessian matrix according to the quadratic terms of the objective function.

Step 3. Solve the QP subproblem to find the search direction.

Step 4. Perform the linear search to define the step size.

Step 5. Update the Hessian matrix and the solution.

Step 6. Verify convergence.

Step 7. If the local minimum is found, then stop the problem, otherwise return to step 3.

3 SIMULATION RESULTS

Base Case: We will start by showing the results obtained in the base case, since it is our starting point for implementing production optimization strategies and improving the performance of smart completions. It should be remembered that in this case all parameters of the devices remain constant over time, and that their orifices have a flow area (Control Trajectory) of 100%, to evaluate the production conditions of the well. Figure 4(a) represents the orifice size of the device of each zone. The production conditions, the oil and water production flow rate, of each zone as a function of time are shown in Fig. 4(b); It can be observed that the most permeable zone (Zone B) controls the production in the well, limiting Zone A, this is the clear example of commingled production where two zones with different petrophysical properties, such as pressure and permeability, are produced by a single well. Zone B with the highest production potential is limiting Zone A, preventing the zone from producing at its maximum potential, leaving a large amount of oil remaining in the reservoir without being produced, resulting in the anticipated end of the productive life of the well. Zone B, being the most permeable, can produce more easily and faster all the fluids present, consequently suffers an early water breakthrough, a sudden increase in water production, and an accelerated decline in oil production, otherwise it happens in Zone A, where being so limited can produce oil at a very low but almost constant flow rate and during the 10 years of injection process, the water front does not reach the producer well, resulting in zero production of water. The total water production from the well is provided in its entirety by Zone B.

Controlled Case: due to the impetuous need to solve the problem described in the base case, the optimization of the control trajectories of the devices of each zone was carried out. In order to perform such optimization, the SAO strategy and the SQP algorithm described in previous sections were used, and five control cycles were defined over the 10 years of productive life; the purpose of this optimization is to control the apertures of each device and to react to current production conditions, which may decrease in size when water (or gas) breakthrough occurs, when there is a high production of water, and in the case of a retreat of the water or the need to produce a considerable amount of oil it can increase the size of its flow area. When performing the base case optimization, we obtained abrupt variations in the control trajectories, which led us to implement a smoothing technique to reduce these variations. The smoothing technique consists in applying a penalty to the control variables in the objective function to mitigate the jump of the variable in each control cycle, making the change in the size of the variable is not very abrupt and can be controlled variations in control trajectories. For this reason, the controlled case was divided in two cases, controlled case 1 (CC1) and controlled case 2 (CC2); where the case CC1 represents the optimized controlled case without the smoothing technique, and the case CC2 is the optimized controlled case with the smoothing technique applied to the optimization.

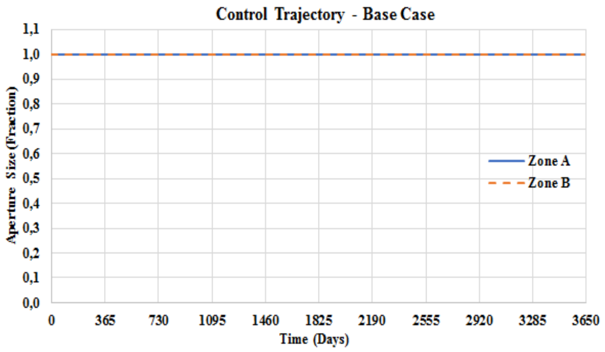

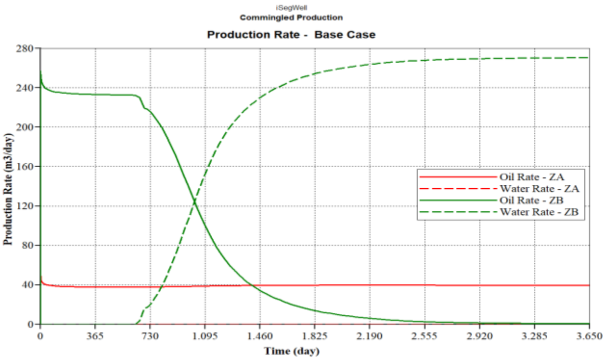

(a) **(b)**

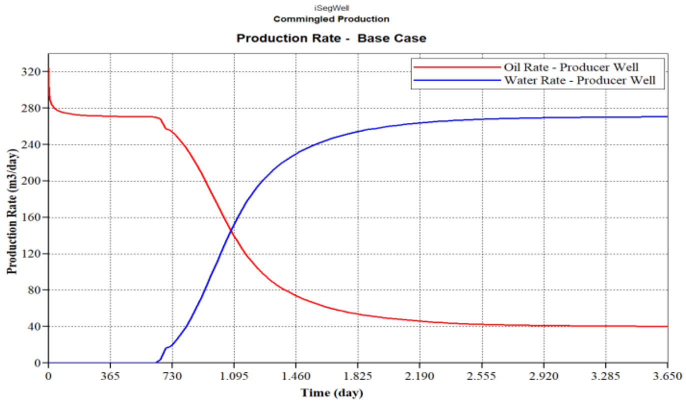

(c)

Figure 4. Production rates and control trajectories at base case. (a) Control trajectories of the devices in each zone. (b) Oil and water rate at each zone. (c) Oil and water rate of producer well

Controlled Case 1: here we present the results obtained by optimizing the variables for the first time. Figure 5(a) shows the abrupt variations in the size of each device, in the figure it can be seen how the orifice of the device installed in Zone A starts with a size of approximately 11% while the device of Zone B starts with a higher value, in this case the optimization process is prioritizing the production of the zone with greater potential, while reducing to a minimum value the production of the less permeable zone; Already to the 730 days of initiated the production, the device of Zone B undergoes an abrupt decrease in the size of its orifice due to the water breakthrough days ago and the increase in water production, as can be seen in Fig. 5(c), since Zone A is suddenly opened to compensate for oil production in the well. Figure 5(c) highlights the abrupt closure of the orifice of device B at 1.825 days due to the sudden and rapid increase in water production and the significant decrease in oil production; In the same way happens in the Zone A, when on day 2.555, the device is closed abruptly due to the sudden and significant increase in water production and the rapid decrease of oil production as shown in Fig. 5(b). In general, the optimization applied in the control variables of the controlled case always tries to decrease the high-water production by reducing the orifice size, as can be seen in Fig. 5(d) on days 730, 1.825 and 2.555.

Controlled case 2: this section presents the results obtained after applying the smoothing technique in the optimization. In this case the optimizations together with the smoothing technique reduced and controlled the variations in the control trajectories (Fig. 6(a)), significantly decreased the amount of water produced and maintained almost constant oil production in the first years of production as can be Fig. 6(d). It is important to emphasize the actions taken by the optimization strategy in counteracting the sudden and rapid increases in the water production after its breakthrough in each zone, decreasing the size of the orifice of each device, this can be seen in Fig. 6(c), where at the third year of production the device of Zone B is closed and controlled by the high production of water; and in Fig. 6(b) the decrease of the production of water of Zone A in days 1.825 and 2.555 can be observed.

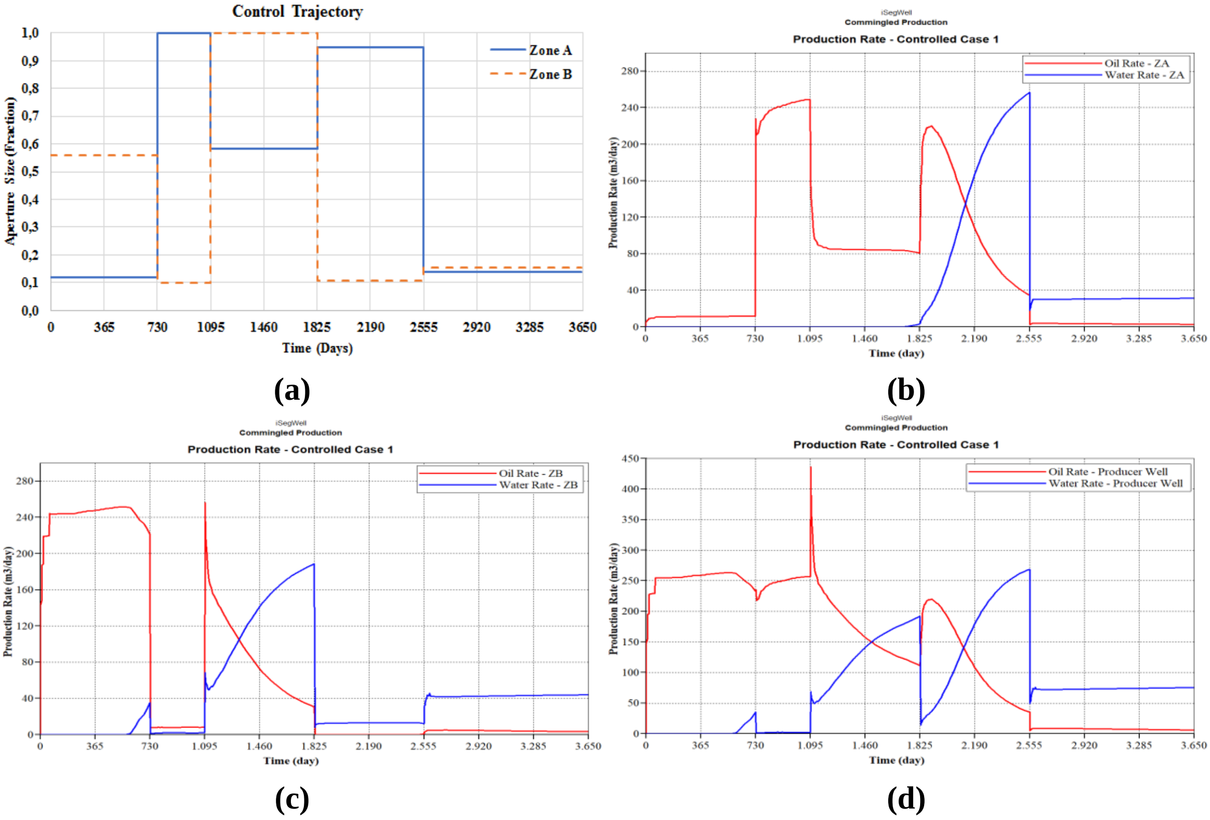

Figure 5. Production rates and control trajectories at controlled case 1. (a) Control trajectories of the devices in each zone. (b) Oil and water rate at zona A (ZA). (c) Oil and water rate at zona B (ZB). (d) Oil and water production of producer well

4 DISCUSION

The base case has the highest water production in the three cases and the least amount of accumulated oil produced, due to the high production of Zone B water and the minimal oil production in Zone A. By performing the optimization of the controlled case, we could increase the accumulated oil and considerably decrease the produced water; Now when applying the smoothing technique, we were able to produce almost the same amount of oil, but we substantially reduced the accumulated water. These good results are reflected in the NPV of each case; When we did the optimization, it was possible to increase the NPV of the reservoir approximately 64,9%, comparing the case CC1 with the base case; and when applying the smoothing technique, we increased the NPV a bit more, about 9,7%, comparing the case CC2 with the case CC1. This leads us to conclude that the optimization technique has a small impact on the production of oil and manages to decrease the variations of the controls. The cumulative production curves are shown in Fig. 7, and the NPV in Table 5.

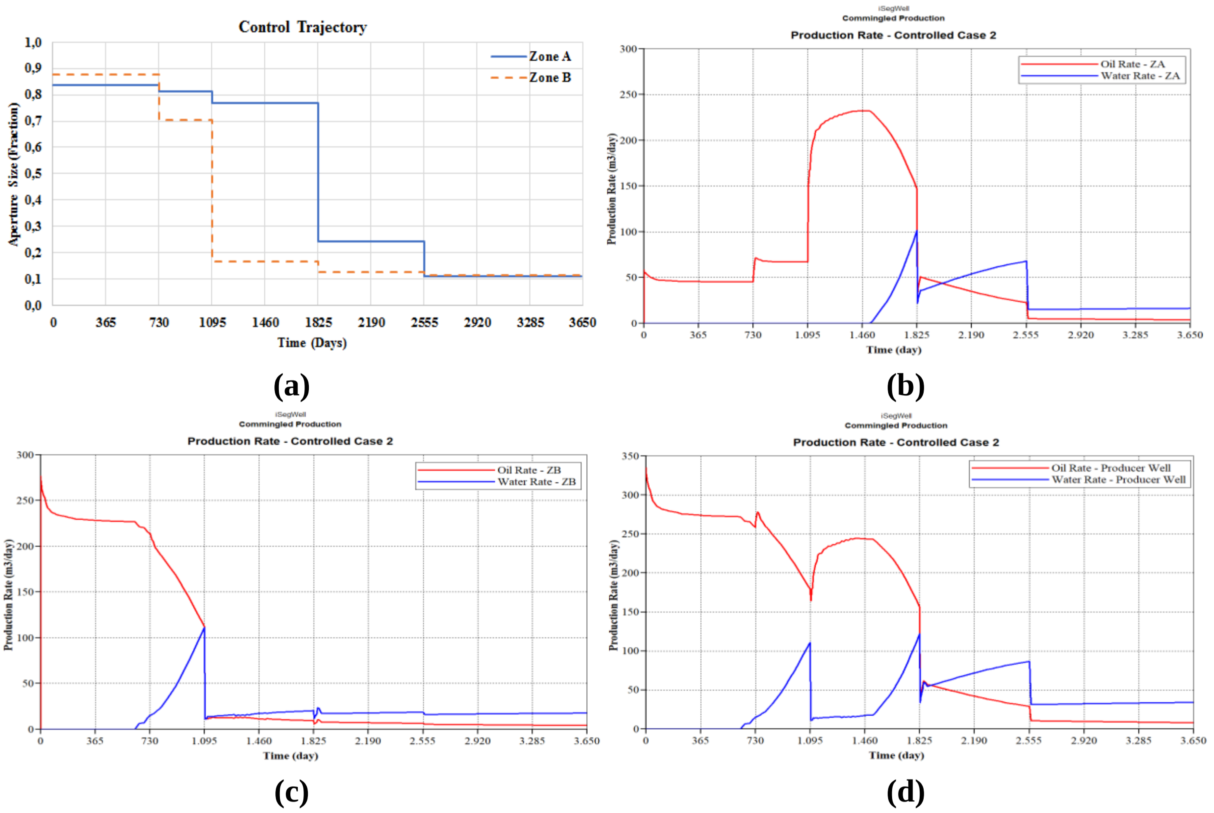

Figure 6. Production rates and control trajectories at controlled case 2. (a) Control trajectories of the devices in each zone. (b) Oil and water rate at zona A. (c) Oil and water rate at zona B. (d) Oil and water production of producer well

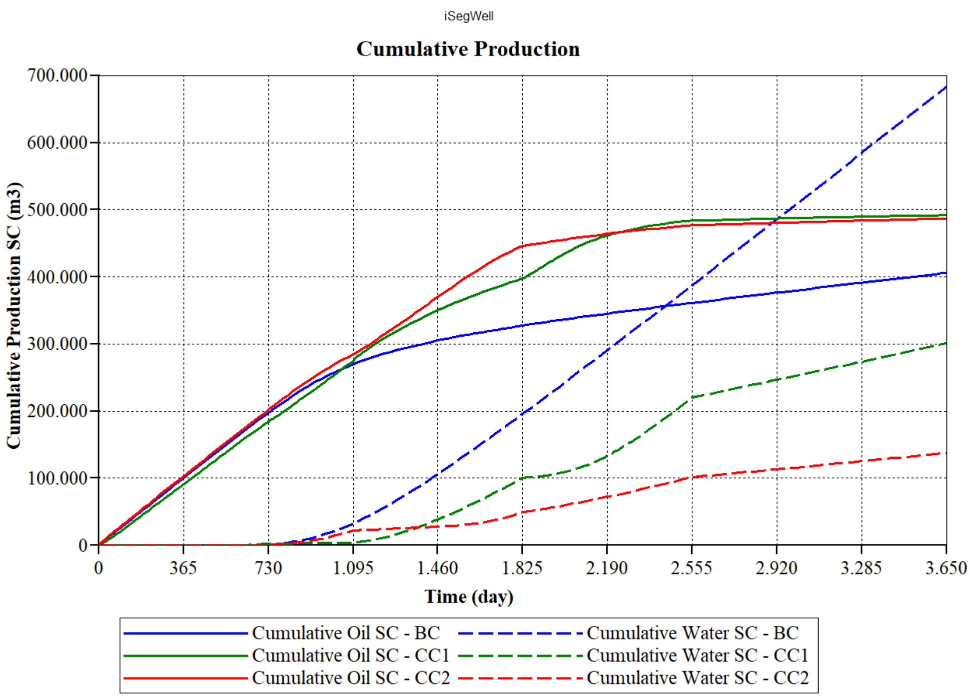

Figure 7. Water and oil cumulative production for each studied case

Table 5. Total cumulative production and final NPV of each case

Case	Cumulative oil (m^3)	Cumulative Water (m^3)	NPV (10^6 \$)
Base	406.091	683.292	28,47
CC1	492.147	300.917	46,94
CC2	487.096	137.664	51,48

5 CONCLUSSIONS

We model and optimize the control trajectories of the installed devices in each zone as close as possible to a real well in a case of commingled production.

We attenuate and control the abrupt variations in the control trajectories applying a smoothing technique in the objective function to penalize the project variables.

The smoothing technique applied in the optimization has a very small impact in oil production and a decrease in water production, thereby improving the performance of the controls and increasing the NPV of reservoir considerably.

REFERENCES

Aakre, H., Halvorsen, B., & Werswick, B. (2013). SPE 164348-MS Smart Well With Autonomous Inflow Control Valve Technology. *SPE Middle East Oil and Gas Show and Exhibition*, 1–8.

Al-khelaiwi, F. T., Birchenko, V. M., Konopczynski, M. R., & Davies, D. R. (2010). Advanced Wells : A Comprehensive Approach to the Selection Between Passive and Active Inflow-Control Completions. *SPE Production & Operations*, (August).

Alexandrov, N. M., Dennis, J. E., Lewis, R. M., & Torczon, V. (1998). A trust-region framework for managing the use of approximation models in optimization. *Structural and Multidisciplinary Optimization*, *15*(1), 16–23.

Alsyed, S., & Yateem, K. (2012). SPE 150014 Testing Methodology for Smart Wells Completion toward Attaining Optimal Production Rate Setting for Maximum Hydrocarbon Recovery. *SPE Intelligent Energy International*.

Boone, T. J., Youck, D. G., & Sun, S. (2001). Targeted Steam Injection Using Horizontal Wells With Limited Entry Perforations. *Journal of Canadian Petroleum Technology*, *40*, 25–30.

CMG. (2016a). IMEX User Guide Three-phase, Black-oil Reservoir Simulator. Calgary, Alberta: Computer Modelling Group Ltd.

CMG. (2016b). iSEGWELL User Guide Intelligent Segmented Well. Calgary, Alberta: Computer Modelling Group Ltd.

Eldred, M. S., Giunta, A. A., Collis, S. S., Alexandrov, N. A., & Lewis, R. M. (2004). Second-order corrections for surrogate-based optimization with model hierarchies. In *Proceedings of the*

10th AIAA/ISSMO Multidisciplinary Analysis and Optimization Conference, Albany, NY,, Aug (pp. 2013–2014).

Ellis, T., Erkal, A., Goh, G., Leung, E., Porturas, F., & Vorkinn, P. B. (2010). Inflow Control Devices — Raising Profiles. *Oilfield Review Winter*, *21*(4), 30–37.

Giunta, A. A., & Eldred, M. S. (2000). Implementation of a trust region model management strategy in the dakota optimization toolkit. *American Institute of Aeronautics and Astronautics*, (c).

Glandt, C. A., & E, S. I. (2005). Reservoir Management Employing Smart Wells : A Review. *SPE Drilling & Completion*.

Hibiki, T., & Ishii, M. (2003). One-dimensional drift-flux model and constitutive equations for relative motion between phases in various two-phase flow regimes. *International Journal of Heat and Mass Transfer*, *46*, 4935–4948. https://doi.org/10.1016/S0017-9310(03)00322-3

Horowitz, B., Bastos, M. S. A., & Mendonça, V. (2013). Surrogate based optimal waterflooding management. *Journal of Petroleum Science and Engineering*. https://doi.org/10.1016/j.petrol.2013.11.006

Jasen, J. D. (2001). Smart wells. *Shell E&P Technology Applications and Research*, 1–11.

Leemhuis, A. P., Belfroid, S. P. C., Alberts, G. J. N., & Science, T. N. O. (2007). Gas Coning Control for Smart Wells. *SPE Annual Technical Conference and Exhibition*, 1–8.

Meshioye, O., Mackay, E., Ekeoma, E., & Chukuwezi, M. (2010). SPE 136996 Optimization of Waterflooding Using Smart Well Technology. *34th Annual SPE International Conference and Exhibition*.

Oliveira, L. C. de. (2013). *Estratégia híbrida aplicada ao gerenciamiento ótimo de reservatórios*. PhD thesis, Universidade Federal de Pernambuco.

Perkins, T. K. (1993). Critical and Subcritical Flow of Multiphase Mixtures Through Chokes. *SPE Drilling & Completion*.

Perry, R. H., & Green, D. W. (2007). Perry's Chemical Engineers' Handbook. (R. Perry, D. Green, & J. Maloney, Eds.) (7th ed.). New York: McGraw-Hill.

Rahman, J., Allen, C., & Bhat, G. (2012). SPE 150850 Second-Generation Interval Control Valve (ICV) Improves Operational Efficiency and Inflow Performance in Intelligent Completions. *North Africa Technical Conference and Exhibition*, (Icv).

Sefat, M. H., & Muradov, K. (2013). SPE 167453 Field Management by Proactive Optimisation of Intelligent Wells - A Practical Approach. *SPE Middle East Intelligent Energy Conference and Exhibition*, 1–15.

Soprano, A. B., Ribeiro, G. G., Silva, A. F. C., & Maliska, C. R. (2010). Solution of a one-dimensional three-phase flow in horizontal wells using a drift-flux model. *Mecánica Computacional*, *XXIX*, 8767–8779.

Vanderplaats, G. N. (1984). Numerical optimization techniques for engineering design: with applications. New York (N. Y.): McGraw-Hill Ryerson, Limited.

Williamson, J. R., Bouldin, B., & Purkis, D. (2000). SPE 64280 An Infinitely Variable Choke for Multi-Zone Intelligent Well Completions. *SPE Asia Pacific Oil and Gas Conference and Exhibition*.